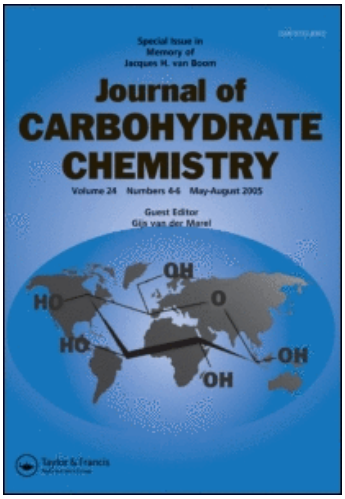

Journal of Carbohydrate Chemistry

Publication details, including instructions for authors and subscription information:
http://www.informaworld.com/smpp/title~content=t713617200

Structural Studies of Antarctic Fish Antifreeze Glycoproteins by One- and Two-Dimensional NMR Spectroscopy

Kilian Dill[a]; Lihua Huang[a]; Daniel W. Bearden[a]; Robert E. Feeney[b]
[a] the Department of Chemistry, Clemson University, Clemson, SC [b] the Department of Food Science and Technology, University of California, Davis, CA

To cite this Article Dill, Kilian , Huang, Lihua , Bearden, Daniel W. and Feeney, Robert E.(1992) 'Structural Studies of Antarctic Fish Antifreeze Glycoproteins by One- and Two-Dimensional NMR Spectroscopy', Journal of Carbohydrate Chemistry, 11: 4, 499 — 517
To link to this Article: DOI: 10.1080/07328309208017809
URL: http://dx.doi.org/10.1080/07328309208017809

J. CARBOHYDRATE CHEMISTRY, 11(4), 499-517 (1992)

STRUCTURAL STUDIES OF ANTARCTIC FISH ANTIFREEZE GLYCOPROTEINS BY ONE- AND TWO-DIMENSIONAL NMR SPECTROSCOPY

Kilian Dill,*,† Lihua Huang,† Daniel W. Bearden,† and Robert E. Feeney§

†*the Department of Chemistry, Clemson University, Clemson, SC 29634 and* §*the Department of Food Science and Technology, University of California, Davis, CA 95616.*

Received October 9, 1991 - Final Form February 18, 1992

ABSTRACT

The solution structure of antifreeze glycoproteins (AFGP's) of the polar fish *Tetramatomus borchgrevinki* has been investigated by 2D ^{1}H NMR spectroscopy as well as molecular modeling calculations (MM2). The simple glycotripeptide repeating structure in the shorter AFGP's (fractions 7 & 8) makes the structural analysis amenable. The resonance assignments of AFGP's 7 & 8 were determined by two-dimensional NMR techniques (COSY, Relayed-COSY, Phase Sensitive DQCOSY, NOESY). Information about the protein secondary structure was obtained by the coupling constants between the back-bone amide and α-carbon protons (obtained by phase sensitive COSY). Additional three dimensional constraints were obtained from NOESY through-space connectivities. The three dimensional solution structures of several AFGP's glycotripeptide fragments were based on MM2 calculations. The model structure was compared with the experimental data. Exchange rates of amide protons measured by dynamical spectroscopy show that the threonine and some of the alanine amide protons have two different and distinct exchange rates. GalNAc and the C-terminal Ala' amide protons appear to show relatively

slow exchange rates. The results suggest that the amide protons are not involved in any strong intramolecular hydrogen bonding.

INTRODUCTION

Polar fishes live in an environment where the temperatures often drop below -1.8 °C,[1-3] which is the equilibrium temperature of salt water in polar seas. In most non-polar fishes, sodium chloride is the principal electrolyte present in the blood and is responsible for 85% of the freezing point depression.[4] The remainder of the freezing point depression is due to small amounts of other salts and nutrients present (for instance, potassium salts, calcium salts, urea, glucose, globular proteins, and free amino acids).[5] In polar fishes, the concentration of sodium chloride and other substances in body fluids is elevated, but this accounts for only less than two thirds of the observed freezing point depression.[6,7] The much lower freezing point of polar fish fluids is due to the existence of a class of glycoconjugates called antifreeze glycoproteins (AFGP's).[1,8]

The antifreeze glycoproteins exert the large freezing point depressions by a non-colligative mechanism which is presently considered to be a kinetic adsorption-desorption of AFGP at the ice-solution interface.[3] On a mass basis, they are as effective as sodium chloride in depressing the freezing point of water. On a mole basis, however, they depress the freezing point by 200-300 times more than that expected on the basis of colligative relationships alone.[9,10] These glycoproteins appear to not only lower the freezing point in a non-colligative manner, but they show the expected small colligative effect on the melting point of the solid phase.[2]

Antifreeze glycoproteins are a collective name for a family of eight closely related glycoproteins. Their molecular masses range between 2,600-34,000 Da (from 14 to 300 amino acids).[1,8,11] The AFGP's derived from arctic and antarctic fishes are almost identical in composition and their structures are simple; they exist as a mixture of simple glycotripeptide polymers of varying length that contain a disaccharide[10,11] as shown below:

$$(\text{Ala-Ala-Thr})_n$$
$$|$$
$$\beta\text{-Gal}(1\text{-->}3)\alpha\text{-GalNAc}$$

The longer AFGP's (fractions 1-5) have a homogeneous repeating structure, while the shorter AFGP's (fractions 6, 7, & 8) have some of the

alanine residues replaced by proline residues. The sequences of AFGP 7,8 from *Tetramatomus borchgrevinki* are shown below.[13]

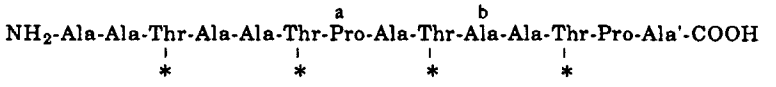

8

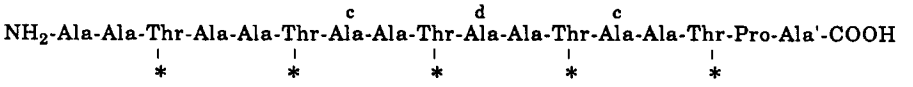

7

* = β–Gal(1-->3)α–GalNAc

a Ala:Pro = 3:7
b Ala:Pro = 8:2
c Ala:Pro = 2:1
d Ala:Pro = 9:1

These shorter AFGP's have characteristics different from those of the longer ones. The shorter ones are the major antifreeze components of the blood serum, comprising approximately three-quarters of the total weight present in the serum.[14] Although they have only one-fourth the activity on a weight basis (or approximately one-twentieth on a mole basis), they provide nearly half of the total antifreeze activity because of their much higher concentration. But in the extracts of tissues they are the only type found in easily recognizable amounts.[15] The shorter AFGP's also function cooperatively with the longer ones under certain conditions.[15]

In this paper we present two-dimensional NMR data that gives insight into the solution structure of the antifreeze glycoproteins. Furthermore, we present exchange rates for the amide protons as well as molecular modeling calculations that support our structures of these glycoproteins. The data suggests that little strong internal hydrogen bonding exists involving the amide protons of these glycoproteins. The amide proton of GalNAc shows the slowest exchange rate and this residue may be the only one involved in weak hydrogen bonding (if at all).

RESULTS AND DISCUSSION

The small number of proline residues present in our sample affect the three dimensional structure of the glycoprotein and our lack of spectral resolution prevents a full sequential assignment of the spectra. In addition, the exchange of some of the amide protons also increase the linewidth of the Ala and Thr amide proton resonances at pH ~7.0. Therefore, the spectral data that we obtained are considerably different from that obtained by Bush and Feeney[16] for AFGP's 1-4 obtained from *T. borchgrevinki* (especially in the amide proton region which in their case was determined at low pH) but similar to that published by Rao and Bush[17] for AFGP 8 obtained from *B. saida* which contains two uniformly substituted proline residues in the amino acid sequence.

Assignment of the ^{1}H NMR spectrum of AFGP's: The resonance assignment in the ^{1}H NMR spectrum of AFGP's was obtained by standard procedures:[18,19] COSY, RCOSY, and PS-DQCOSY spectroscopy were used to identify intra-residue, through-bond connectivities, and NOESY spectroscopy was used to identify neighboring residues by through-space ($\leq$ 5 Å) connectivities.

Examples of 2D NMR spectra are shown in Figs. 1-3. A number of resonances can readily be assigned based upon their positions in uncrowded regions of the spectra. For instance, the methyl protons of Ala (H^β) and Thr (H^γ) (1.32- 1.44 ppm), the acetamido proton of GalNAc (2.03 ppm), and the anomeric proton of GalNAc (about 4.95 ppm) are readily detected and assigned. The amide portion of the spectrum can be used to corroborate our findings and make further assignments. The Ala and Thr amide proton resonances, and GalNAc acetamido proton resonances were identified by comparing COSY, one step RCOSY, and NOESY 2D NMR plots of the amide proton cross-peak finger print region (Fig. 1). For example, the amide protons of the Ala residues will exhibit a cross-peak with the methyl protons (H^β) in the RCOSY spectrum via the H^α. Furthermore, the amide proton of GalNAc shows a cross-peak with the GN-H1 (GN1) and GN-H3 (GN3) in the RCOSY spectrum (because of relay through GN2) and a cross-peak with the acetamido methyl group in the NOESY spectrum. After the assignment of the amide protons, the other protons of Ala and Thr were readily assigned (but not sequentially). The cross-peaks for GN2/GN3, GN3/GN4 and GN4/GN5 overlap, but the detailed analysis of the phase

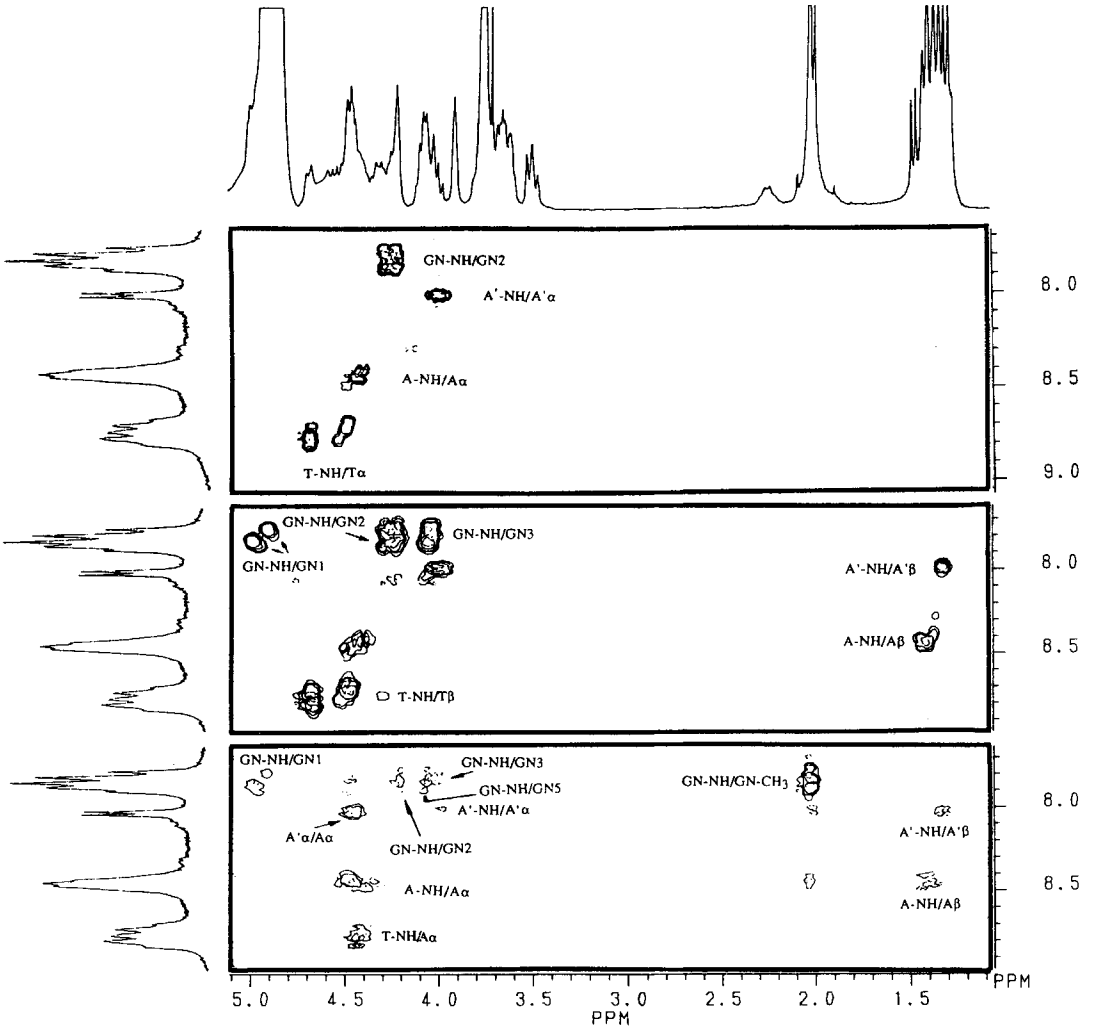

Fig. 1. Fingerprint (amide proton) regions of the 2D-COSY (upper), 2D-RCOSY (middle) and 2D-NOESY (lower) plots of AFGP's 7 & 8 in 90% H_2O.

sensitive COSY and Double Quantum COSY spectra also determined their positions. The Gal H1 resonance assignment was initiated with H2, because this resonance is well separated from other proton resonances. Difficulties arose with the assignment of this carbohydrate molecule because the cross-peaks for G3/G4 and G4/G5 overlap and the vicinal coupling constants are small.[20]

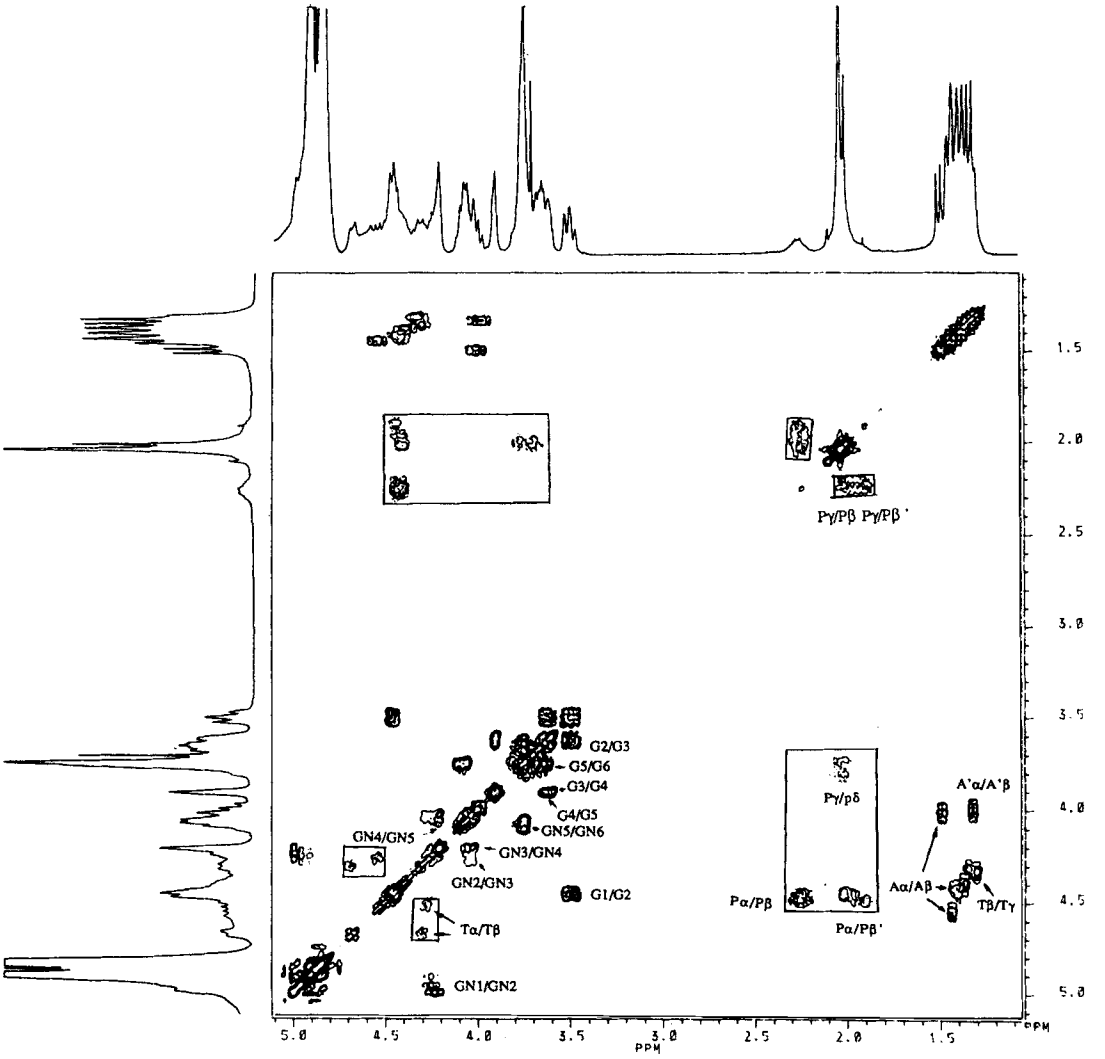

Fig. 2. The 2D-COSY plot of AFGP's 7 & 8. Cross-peaks in boxes are plotted at a lower level with a scaling factor of 8.

We were able to assign all the resonances of the C-terminal Ala' residue, and the assignments are in agreement with those published by Rao and Bush[17] for AFGP 8 from *B. saida*. The Ala' amide proton resonates at 7.980 ppm and exhibits a cross-peak (in the COSY contour plot) with a proton at 3.99 ppm (H^{α}), and a cross-peak (in the RCOSY contour

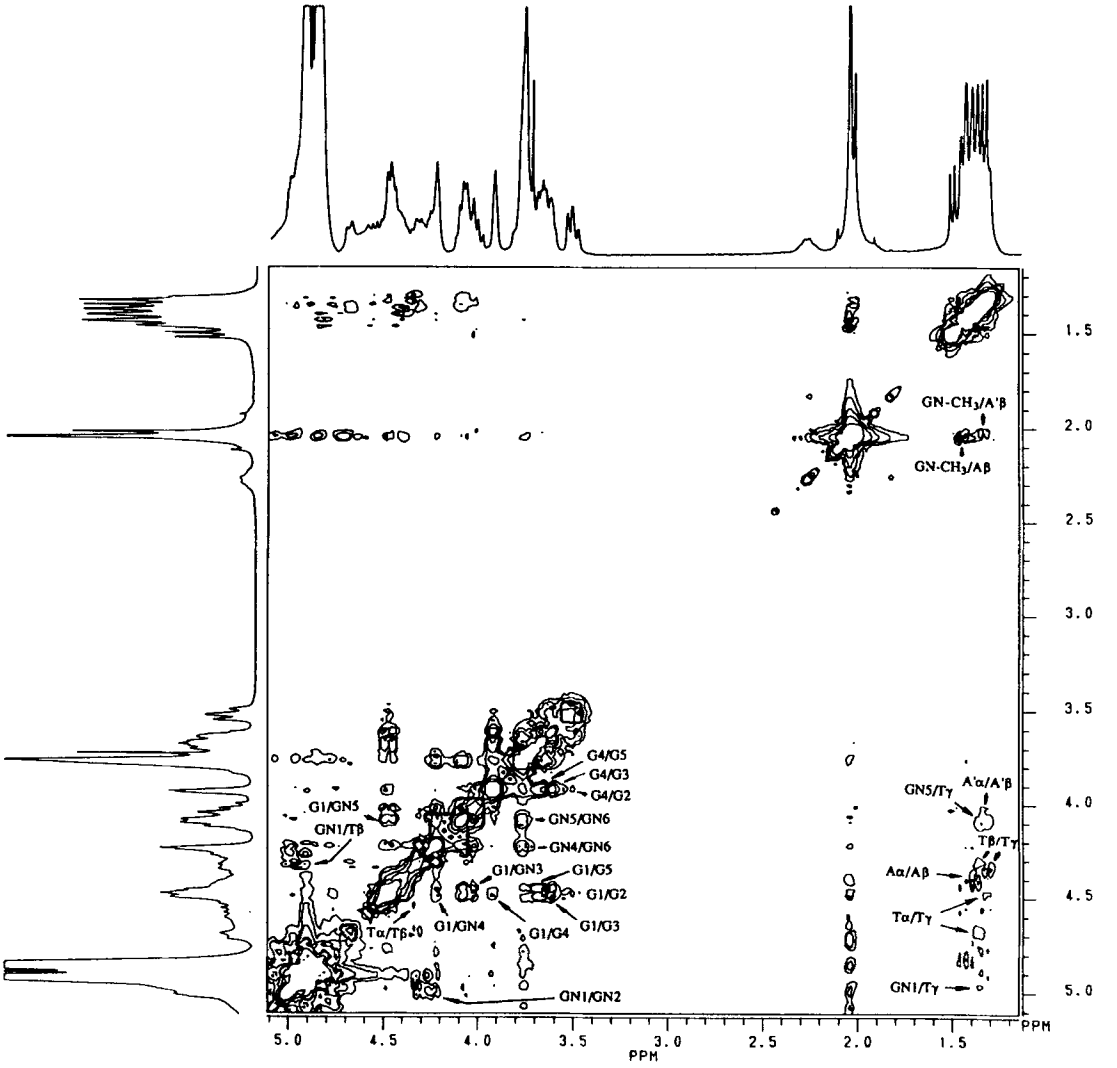

Fig. 3. The 2D-NOESY spectrum of AFGP's 7 & 8 using a mixing time of τ_m = 500 ms.

plot) with a proton at 1.326 ppm (H^{β}). A list of the assignments are given in Table I. Although GalNAc and Thr residues present represent at least two distinct structures; the repeating units of Ala-Thr-Ala and Ala-Thr-Pro, these also give many local structural perturbations as judged by the number of resonances present for a particular residue. This is evident in the amide region of the spectrum where a large degree of chemical shift

Table I. Chemical Shift Data for AFGP's 7 & 8.

residue	Chemical shift (ppm)							
	NH	$C^{\alpha}H$/H1	$C^{\beta}H$/H2	$C^{\gamma}H$/H3	$C^{\delta}H$/H4	H5	H6	Amide methyl
Gal	--	4.47	3.50	3.64	3.91	3.67	3.75	--
GalNAc	7.747	4.966	4.261	--	4.22	--	3.75	2.037
	7.786	4.92	4.26					
	7.812	5.01	4.25					
	7.842	5.00	4.24					
Ala'	7.980	3.99	1.326					
Ala	8.391	4.42	1.443					
	8.432	4.40	1.388					
	8.738	4.54	1.439					
	--	4.03	1.508					
Thr	8.651	4.48	4.33	1.318				
	8.681	4.50	4.33	1.318				
	8.718	4.69	4.32	1.361				
	8.760	4.68	4.32	1.361				
Pro	--	4.49	2.27, 2.00	2.05	3.77			

non-equivalence is observed for a given residue. Thus, it is not possible to make one-to-one assignments of all cross-peaks in 300 MHz NMR. Furthermore, the absence of a large number of NOE cross-peaks between the amide region and other portions of the spectra (due to fast exchange of some of the amide protons or rapid conformational changes) hinders our resonance assignments and limits some of our molecular structural

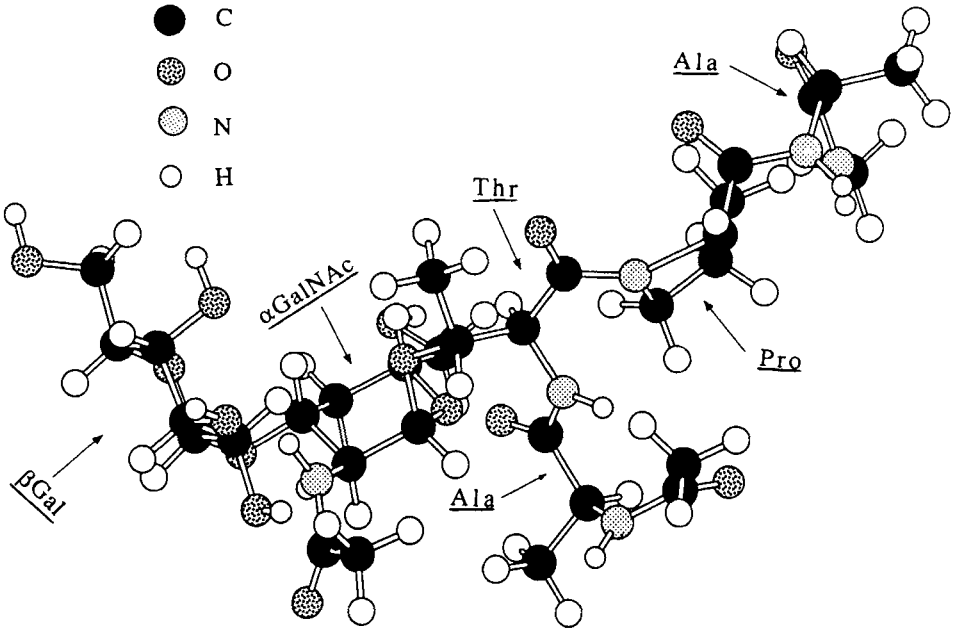

Fig. 4. The ball & stick representation of N-acetyl-Ala-[β-Gal(1->3)α-GalNAc-O]Thr-Pro-Ala-N-methyl amide.

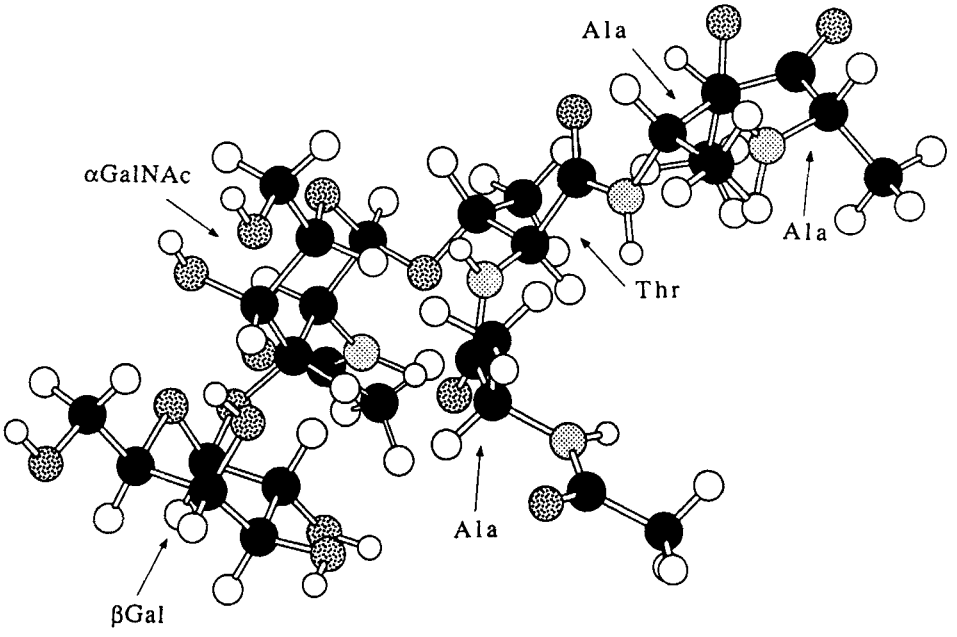

Fig. 5. The ball-stick representation of N-acetyl-Ala-[β-Gal (1->3)α-GalNAc-O]Thr-Ala-Ala-N-methyl amide.

determinations. Although the lack of NOE cross-peaks between the amide region and other regions of the spectrum could be attributed to correlation time, the fact that we observe NOE cross-peaks between GalNAc and the peptide backbone indicates that the former reasoning is more plausible.

The NOE data in Figs. 1 and 3 provide additional information concerning our structures. Note that cross-peaks do exist between GN-CH_3 and Ala H^{β} (and Ala' H^{β}) indicating that these residues are in close proximity (see Figs. 4 & 5). NOE cross-peaks also exist between Ala-NH and GN-CH_3 (Fig. 1), corroborating the structures shown in Figs. 4 & 5. The sequence and protein glycosylation points of the disaccharide can also be confirmed by the NOE data: cross-peaks are observed, as expected, between GN1/Thr H^{β} and G1/GN3.[20] Other intercarbohydrate NOE's that can be observed are G1-GN4 and G1-GN5. Although these may be expected, they do give conformational information about the glycosidic bond (Figs. 4 & 5).

Measurement of the exchange rates of amide protons: The relative exchange rate of amide protons depends upon their exposure to bulk water molecules and whether they are involved in inter-residue hydrogen bonding within the molecule; both contribute to slower amide exchange rates. Thus, the measurement of the amide hydrogen exchange rate can indirectly be used to judge whether or not a hydrogen bond exists.

One method for the qualitative evaluation of the solvent exposure (or hydrogen bonding) of an amide proton is the measure of the temperature dependence of the chemical shift of the amide proton resonance.[21] Values of $d\delta/dT > .004$ indicate solvent exposure. The temperature dependence of the amide protons of AFGP's 7 & 8 are given in Table II. The qualitative data suggests solvent exposure for all amide protons but there are some differential effects. This result is in agreement with the observation made by Rao and Bush[17] for AFGP 8 from *B. saida*.

Another method for the analysis of solvent accessibility of the amide protons is to compare the amide proton spectra obtained with pre-saturation of the water resonance and the spectra obtained with the suppression of the water resonance by jump and return pulses (Fig. 6); it is apparent that the amide protons of Ala and Thr exchange with water faster than the amide protons of C-terminal Ala' and GalNAc. Although the Jump and Return method does not excite all of the protons in the spectrum equally, the spectral window of interest (7.8 - 8.9 ppm) is relatively narrow and hence the inaccuracies are small. If we change the delay between

Table II. Temperature Dependence of the Chemical Shifts of the Amide Resonances of AFGP's 7 & 8. [a]

Residue	$d\delta/dT$[b]
GalNAc	.0084
Ala	.0094
Ala'	.0114
Thr	.0172

a. Except for Ala', the residues represent the clusters of amino acids or sugar residues.

b. Given in ppm/K

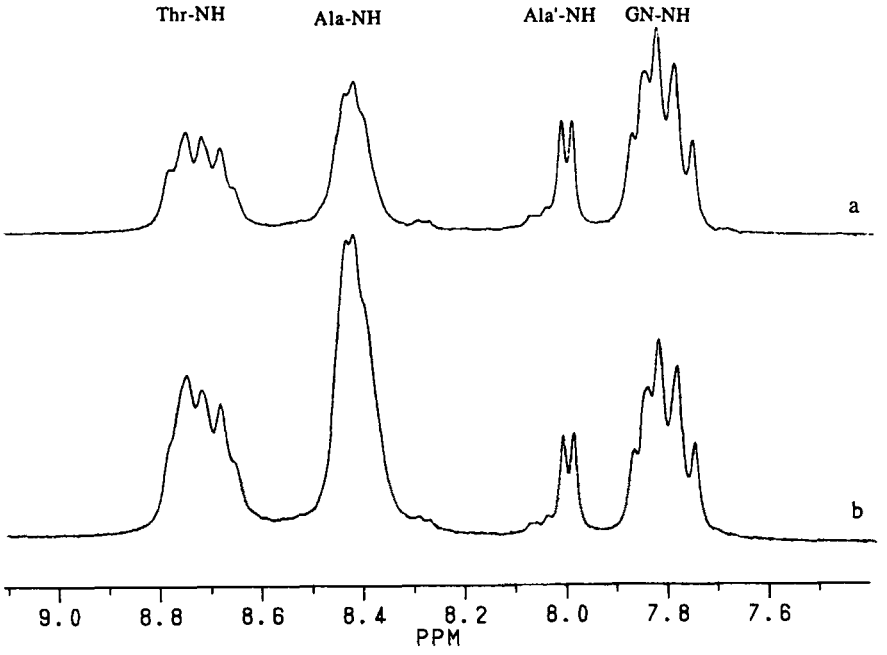

Fig. 6. Amide proton resonance region of ^1H NMR spectrum of AFGP's 7 & 8 in 90% H_2O solution at room temperature (pH = 7.4). The strong water proton resonance was suppressed by selective saturation (a) or the jump and return pulse method(b).

Table III. The Comparison of Peak Intensities of Amide Protons of AFGP's 7 & 8 Using the Various Water Suppression Techniques.

Method	Thr-NH	Ala-NH	Ala'-NH	GalNAc-NH
Jump-return	200	271	46	180
Saturation	113	130	45	176

jump pulse and return pulse several times and the maximum values of the peaks of interest are used, the inaccuracies are negligible. The results are given in Table III.

A further method of analyzing the exchange of amide protons with water molecules is to monitor the spin-lattice relaxation time of the amide protons using selective and non-selective inversion recovery experiments. The non-selective inversion-recovery experiments show that the exchange rate of the C-terminal Ala' and GalNAc amide protons exhibit a relationship for $\ln([M]_z-[M]_z^{\infty})$ that is linear with time (Fig. 7); furthermore, a DANTE pulse sequence (selective-inversion) followed by 180 and 90 degree pulses also gave similar results (Fig. 7). However, in contrast to the results for Ala' and GalNAc, the results for the Thr and Ala amide protons were not the same, as shown in Fig. 7. This indicates that the Thr and Ala amide protons are exchanging at a much faster rate than the Ala' and GalNAc amide protons.

The exchange rates, based upon numerical analyses, can be obtained by non- or selective-inversion recovery experiments based on the above relaxation analysis. The results are shown in Table IV. The Table also includes the ratio of different rates based upon concentrations and the values for the slopes of the plots of $\ln([M]_z-[M]_z^{\infty})$ vs. time shown in Fig. 7. Although we do observe differential amide proton exchange rates for the various species, the difference is not large enough to indicate whether any of these amide moieties are involved in the formation of a strong internal hydrogen bond.

Comparison of Theoretical Calculations and Experimental Results: The structures of repeating units of glycotripeptides composed of Ala-Thr-Ala and Ala-Thr-Pro, obtained by MM2 calculations, are shown in Figs. 4 and

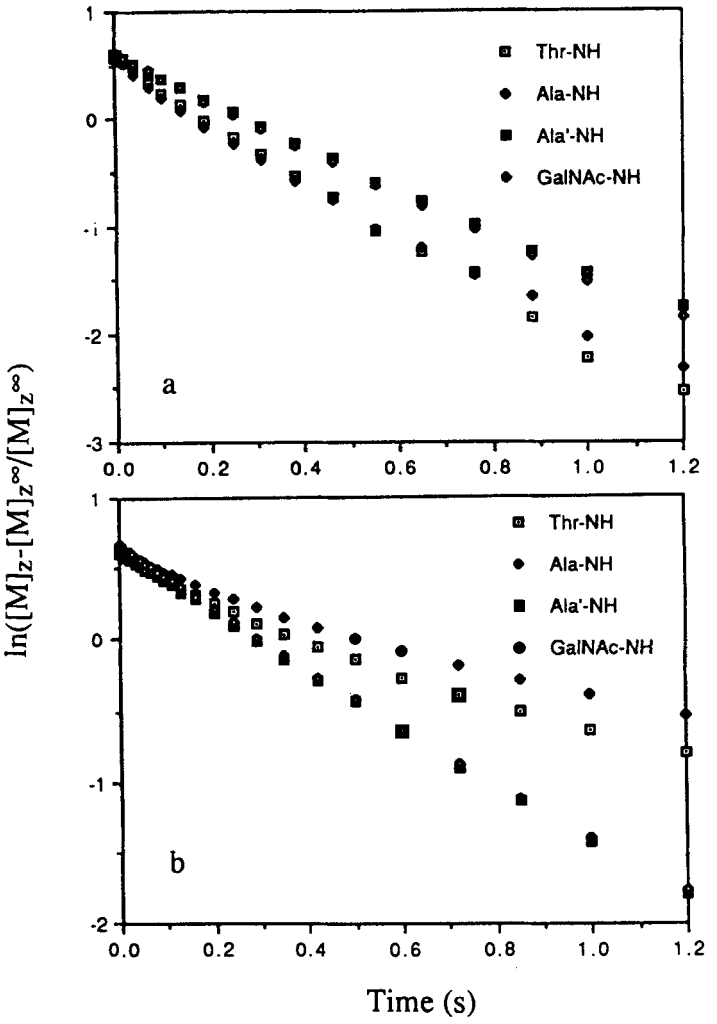

Fig. 7. The semilogarithmic plot of the time-dependent signal (amide proton resonances) intensities from the non-selective inversion recovery experiments. (a) With selective pre-saturation of the water resonance (upper graph); (b) with jump and return pulse to suppress the water proton resonance (lower graph).

Table IV. Kinetic Data Obtained by the Selective Inversion, Non-selective Inversion Recovery Experiments and Non-linear Least Square Fit for the Amide Protons of AFGP's 7 & 8.

	Thr	Ala	Ala'	GalNAc
$\lambda_1(s^{-1})^a$	5.768±0.013	5.205±0.589	3.010±0.263	3.320±0.236
$\lambda_2(s^{-1})^a$	23.08±0.51	13.46±0.58	--	--
Ratio(A_1/A_2)	3.66±0.12	0.78±0.30		
Round off	4:1	1:1		
$slope_1(s^{-1})^b$	2.670±0.181	2.607±0.006	2.065±0.028	2.132±0.036
$slope_2(s^{-1})^c$	1.222±0.060	1.015±0.044	2.055±0.011	2.052±0.035

a. Using the $[NH]_z = A_1 e^{-\lambda_1 t} + A_2 e^{-\lambda_2 t} + [NH]_z^{\infty}$ for selective inversion experimental data fitting, where $\lambda_i = \rho_i + k_{i,ex}$ if neglecting cross relaxation.

b. 180-τ-90 experiments using pre-saturation of water.

c. 180-τ-90 experiments of the suppression of water by jump and return pulse.

5. Note that for the calculations the model compounds used have both the C- (N-methyl amide) and N-terminal (N-acetyl) blocked. Table V gives the comparison of the theoretical data and the experimental results for the dihedral angles between the amide protons and H^{α} or GN2; they are in good agreement. The experimental results of dihedral angles were based upon the coupling constants that were obtained and then converted to the dihedral angles via the Karplus relationship.[22]

As shown above, our experimental results and theoretical data are in good agreement. They show that show that two distinct structures exist for AFGP's 7 & 8 from T. borchgrevinki. Furthermore the kinetic rate data for the amide protons indicates that no strong intramolecular hydrogen bond

Table V. The Coupling Constants for Amide Protons and the Dihedral Angles for NH-H^{α}.

		Karplus Equation		Model	
NH (ppm)		$^3J_{HN\alpha}$(Hz)	Θ(Deg.)	Ala-Thr-Ala	Ala-Thr-Pro
GalNAc	7.748	9.3	166	171	
	7.789	9.3	166		
	7.808	9.3	166		159
	7.842	9.3	166		
Thr	8.651	8.8	162		159
	8.681	8.8	162		
	8.718	8.3	154	154	
	8.760	8.3	154		
Ala	8.432	5.7	132	123	
	8.391	5.2	128	121	
Ala'	7.990	6.4	137		149

(involving an amide moiety) exists in this glycoprotein. We cannot however rule out the existence of any weak internal hydrogen bonds. Further studies are under way to investigate the solution structure and function of these glycoproteins.

EXPERIMENTAL

A mixture of antarctic fish antifreeze glycoproteins 7 & 8 from *T. borchgrevinki* was prepared as described previously.[13] The NMR sample contained approximately 25 mg AFGP's 7 & 8 in 90% H_2O/10% D_2O, pH 7.40.

All NMR spectra were recorded on a Bruker AC300E at room temperature, except for the temperature studies of the amide protons. For the selective inversion experiments, we used a selective DANTE pulse

sequence[23] to invert the spins of interest in conjunction with the jump and return method[24] to suppress the water resonance. The non-selective inversion experiments were accomplished by the pre-saturation of water resonance or by a jump and return pulse in order to suppress the intense water resonance. Furthermore, all two dimensional spectra were recorded at room temperature in H_2O with the suppression of the water resonances by one of the methods described above. Typically, 512 increments of 2K data points or 256 increments of 1K data points were collected per experiment, yielding, after zero filling, spectra with a digital resolution on the order of 2-5 Hz/pt in each dimension. A pure sine bell window was applied in both F_2 and F_1 dimensions.

Three dimensional structures of the small glycotripeptide units were determined using the PC Model program (Serena Software, Bloomington, IN) with a dielectric constant of 72.0 to simulate an aqueous environment. The energy minimization is based on the MM2 force field calculations of Burket and Allinger.[25]

Relaxation Analysis. Several factors prevent the detailed analysis of chemical exchange in our system from being entirely straightforward. The primary complication comes from the cross-relaxation between amide protons and other protons (e.g. α-protons) in the molecule. However, recent results indicate that under our conditions neglecting cross-relaxation would only produce a minimal error.[26]

Another problem is the spectral overlap in the amide region of the spectrum. We have assigned the four regions observed in the amide region (see below) to specific amino acid and GalNAc residues as described in the following sections, but sequential assignments have not been made. We, therefore, consider these regions (or clusters) to represent an average over the whole glycoprotein molecule, giving an "effective" chemical exchange rate for each cluster which is a composite for all similar amides in the molecule. Because of this averaging, non-exponential time-dependent intensities are interpreted as being due to large differences in the chemical exchange rates within a cluster.

The details of the kinetic processes involved in amide proton/water proton exchange presents a further complication. Many schemes can be written down for the details of the actual mechanism of exchange, the primary candidate being the acid and base catalyzed processes:[27,28]

1. Acid catalyzed mechanism:

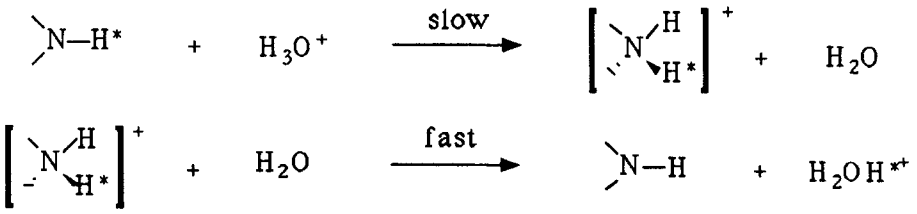

2. Base catalyzed mechanism:

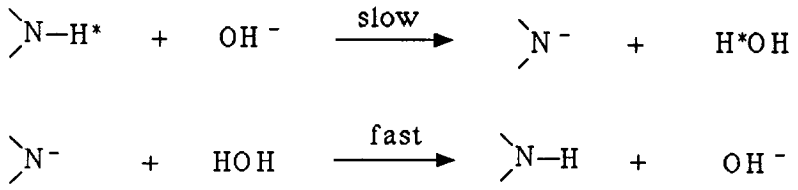

According to the proposed acid and base catalyzed mechanisms, we can write the exchange rate equation of an amide proton and water protons as follows, based upon the rate limiting step.

$d[NH]/dt = k_A[H^+][NH^*] + k_B[OH^-][NH^*]$, and

$d[NH]/dt = k_{ex}[NH^*]$; where $k_{ex} = k_A[H^+] + k_B[OH^-]$.

$= -k_{ex}[NH] + C$

If the amide protons have different exchange rates, the general rate equation can be obtained

$d[NH]/dt = -\Sigma k_{i,ex}[NH]_i + \Sigma C_i$

where $[NH] = \Sigma [NH]_i$.

This scheme and others lead to higher order exchange-rate equations which must be simplified by a host of ambiguous assumptions in order to be useful. We have taken the simplification to its most extreme form and have analyzed the data in terms of simple two-site exchange with a pseudo-first-order rate constant.

A final complication occurs because of the experimental difficulty of achieving water signal suppression in our 90% H_2O/10% D_2O sample. The effect of chemical exchange with amide protons on the size of the water resonance is small, so any attempt to measure intensity changes in the water resonance is futile. We have made our measurements using the

amide portion of the spectrum only, and have used two techniques (presaturation and jump and return) to reduce the intense water resonance to manageable levels as described in the Experimental Procedures.

REFERENCES

1. R. E. Feeney and Y. Yeh, *Adv. Protein Chem.*, **32**, 191 (1978).
2. A. L. DeVries, *Phil. Trans. R. Soc. Lond.*, **B304**, 575 (1984).
3. R. E. Feeney, T. S. Burcham and Y. Yeh, *Ann. Rev. Biophys. Chem.*, **15**, 59 (1986).
4. M. S. Gordan, B. N. Andur and P. F. Scholander, *Biol. Bull. Mar. Biol. Lab.*, **122**, 52 (1962).
5. W. T. W. Potts and G. Parry, *Osmotic and Ionic Regulation in Animal*, Vol. 19, Int. Series of Monographs on Pure and Applied Biology and Zoology; Pergamon Press, New York, 1964.
6. A. L. DeVries in *Animals and Environmental Fitness*; R. Gilles, Ed.; Pergamon Press: Oxford, 1980, pp 583-607.
7. D. T. Osuga and R. E. Feeney, *J. Biol. Chem.*, **253**, 5338 (1978).
8. A. L. DeVries in *Biochemical and Biophysical Perspectives in Marine Biology*, Vol. 1; J. S. Sargent and D. W. Mallins, Eds.; Academic Press: London, 1974, pp 289-330.
9. A. L. DeVries and D. E. Wohlschlag, *Science*, **163**, 1074 (1969).
10. A. L. DeVries, *Science*, **172**, 1152 (1971).
11. R. E. Feeney, *Int. J. Pept. Protein Res.*, **19**, 215 (1982).
12. S. K. Komatsu, A. L. DeVries and R. E. Feeney, *J. Biol. Chem.*, **245**, 2901 (1970).
13. R. E. Feeney and D. T. Osuga, *J. Protein Chem.*, **7**, 667 (1988).
14. T. S. Burcham, D. T. Osuga, H. Chino and R. E. Feeney, *Anal. Biochem.*, **139**, 197 (1984).
15. D. T. Osuga, F. C. Ward, Y. Yeh and R. E. Feeney, *J. Biol. Chem.*, **253**, 6669 (1978).
16. C. A. Bush and R. E. Feeney, *Int. J. Pept. Protein Res.*, **28**, 386 (1986).
17. B. N. N. Rao and C. A. Bush, *Biopolymers*, **26**, 1227 (1987).

18. K. Wuthrich, *NMR of Protein and Nucleic Acids*; Wiley, New York, 1986.

19. G. M. Clore and A. M. Gronenborn, *Protein Eng.*, **1**, 275 (1987).

20. K. Dill, S. Hu and L. Huang, *J. Carbohydr. Chem.*, **9**, 863 (1990).

21. H. Kessler, *Angew. Chem. Int. Ed. Engl.*, **21**, 512 (1982).

22. A. Pardi, M. Billeter and K. Wuthrich, *J. Mol. Biol.*, **180**, 749 (1984).

23. G. A. Morris and R. Freeman, *J. Magn. Reson.*, **29**, 433 (1978).

24. P. Plateau and M. Gueron, *J. Am. Chem. Soc.*, **104**, 7310 (1982).

25. U. Burket and N. Allinger, *Molecular Mechanics*, ACS Monograph 177, American Chemical Society: Washington, D.C., 1982.

26. K. Dill, L. Huang and D. W. Bearden, *J. Biomolec. NMR*, in press.

27. S. W. Englander and N. R. Kallenbach, *Q. Rev. Biophys.*, **16**, 521 (1984).

28. G. D. Henry and B. D. Sykes, *Biochem. Cell Biol.*, **68**, 318 (1990).